

Electronic Raman study of Fe^{2+} in FePX_3 ($X = \text{S, Se}$) layered compounds

M. L. Sanjuán,* M. A. Kanehisa, and M. Jouanne

*Laboratoire de Physique des Solides, Université Pierre et Marie Curie,
Tour 13, 4 Place Jussieu, 75252 Paris CEDEX 05, France*

(Received 26 December 1990; revised manuscript received 8 July 1992)

The electronic Raman spectrum of Fe^{2+} ions in FePS_3 and FePSe_3 layered crystals is studied and interpreted in a quasimolecular approach for the iron and its environment. We apply crystal-field theory, and the transition probability for the electronic Raman process is computed as a function of crystal-field parameters and compared with the experimental results. It is found that trigonal distortion from cubic symmetry and spin-orbit coupling are the main contributions. From the spectrum in polarized conditions, the Fe^{2+} site in FePSe_3 and FePS_3 are shown to have trigonal and monoclinic symmetry, respectively. In FePS_3 , the symmetry lowering is explained as a consequence of a magnetostriction effect occurring below the Néel temperature. The evolution of the spectra as temperature is raised is also discussed.

I. INTRODUCTION

Layered materials have raised a great interest in the past few years because of their electrochemical properties. Their structure, with empty "van der Waals" gaps between layers capable of accepting intercalant species (Li, for instance), makes them good candidates for technological applications, such as use as cathode materials in solid-state batteries.

FePS_3 and FePSe_3 are layered compounds of the MPX_3 family, M being a transition metal and $X = \text{S}$ or Se . Their structure, as shown in Fig. 1, derives from that of CdI_2 with the chalcogens occupying the iodine sites and iron and phosphorus pairs the quasioctahedral Cd sites that are left between two anion planes. These interplane spaces are only alternatively occupied, resulting in a quasibidimensional structure of layers formed by FeX_6 or P_2X_6 octahedra weakly coupled through van der Waals forces to adjacent layers.

The unit cell of FePS_3 is monoclinic with $a_m = 5.947$ Å, $b_m = 10.3$ Å, $c_m = 6.722$ Å, and $\beta = 107.16^\circ$. The unit cell of FePSe_3 built on three layers is hexagonal and has $a = 6.26$ Å and $c = 19.82$ Å.¹

The study of the electronic structure is crucial for an understanding of intercalation properties. In these processes the intercalant acts as a reducing species, giving an electron to the cathode and stabilizing itself, in its oxidized form, in the interlayer space. The question arises as to which are the acceptor levels of the cathode that accommodate the excess electrons. Recently, the transition-metal d states have been proposed as such.² This assignment is corroborated by the dependence of the intercalation ability of MPX_3 on the nature of M : Compounds of metals with partially filled d bands intercalate lithium more easily than closed-shell compounds.³ These considerations are supported by the correlation of the optical bands in the region of d - d transitions with band-structure calculations.⁴ MPX_3 compounds show typically two kinds of gaps: a proper one at energies of 6–8 eV, which implies transitions from the valence to the conduction bands, and a "pseudogap" ($E \approx 1$ –3 eV), which has

been shown to be due to charge-transfer transitions from or to d bands.⁵ According to this model, compounds with closed-shell elements will show higher gaps (of interconfigurational type) than compounds with d^n ($n \neq 10$) elements, as actually happens.

If the identification of the $3d$ states as acceptor levels is correct, the magnetic and optical properties should be strongly affected by the intercalation process. This is generally the case, though conclusive results have not yet been presented, mainly because of the difficulty of intercalating lithium in single crystals. Since Raman scattering is very sensitive to the symmetry and interactions acting on the entity contributing to the spectrum, we have studied the Fe^{2+} electronic structure by means of electronic Raman spectroscopy.

The electronic structure of transition-metal compounds has been a subject of great interest in recent years. The main points of discussion are the origin of band gaps and the role played by d states in basic physical properties, such as conductivity and optical spectrum in the ir to uv region.⁶ We shall follow a quasimolecular model, which assumes that the iron and its environment can be treated as if $[\text{FeS}_6]$ or $[\text{FeSe}_6]$ entities were present; Fe-S or Fe-Se interactions are taken into account by adding symmetry-adapted terms (crystal-field potentials) to the free-ion Hamiltonian of the metal. This model is justified by the weak dispersion shown by d bands as well as the relatively strong metal-ligand covalency appearing in electronic-structure calculations.⁴

II. EXPERIMENTAL RESULTS

The Raman spectra were measured in a Jobin-Yvon ISA spectrometer with a U1000 double monochromator and photon-counting detection. A Spectra Physics argon laser was used as a source. From the ratio between Stokes and anti-Stokes phonon intensities, we can estimate the local heating of the sample to be less than 5 K for a laser power of up to 100 mW at the sample surface with spot size of 50 μm . Low-temperature measurements were performed in a SMC-TBT continuous-flow cryostat.

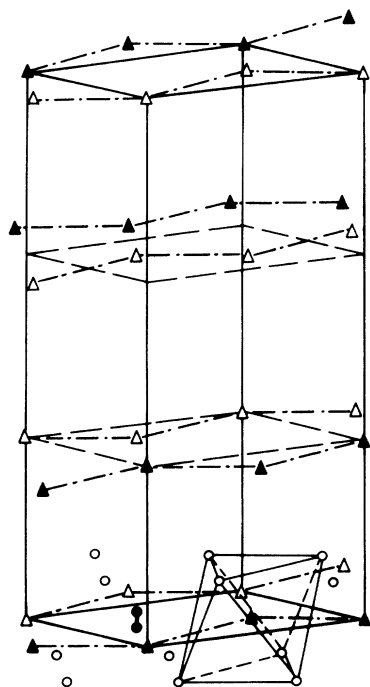
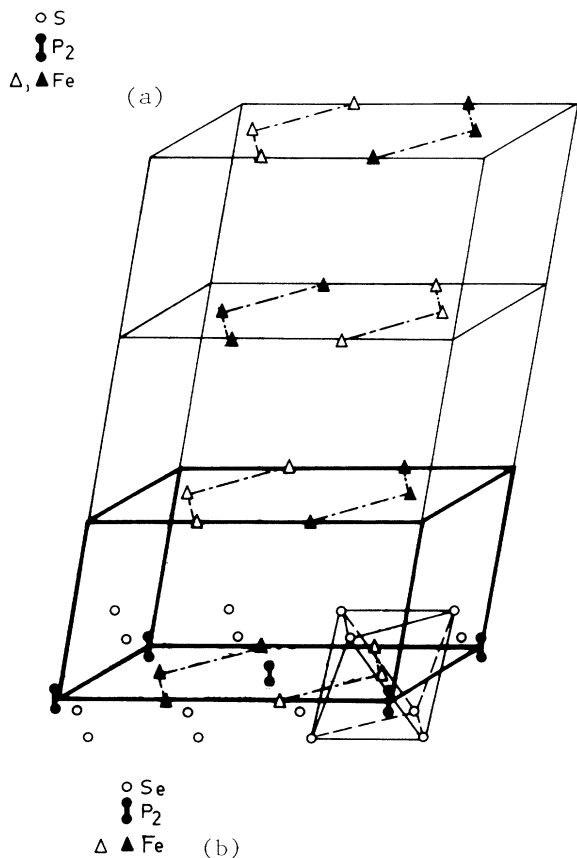


FIG. 1. (a) Crystal structure of FePS_3 showing the monoclinic primitive cell (thick line). (b) Crystal structure of FePSe_3 showing the hexagonal unit cell. In both (a) and (b), the ferromagnetic chains are linked by dashed lines. Spin-up and -down iron ions are indicated by open and solid triangles, respectively.

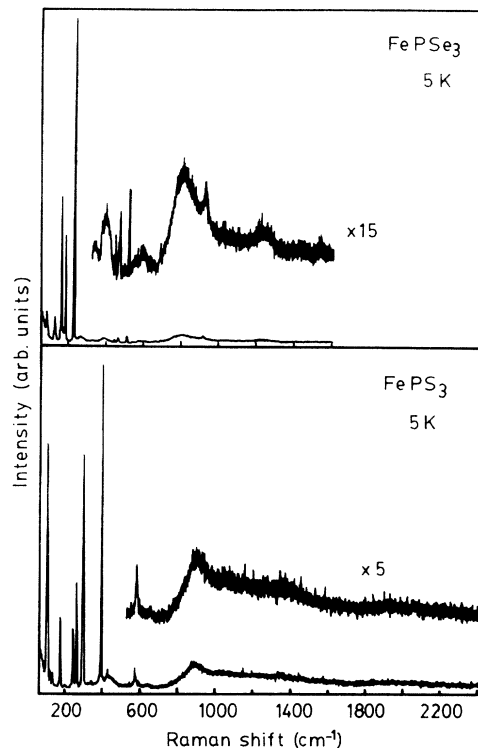


FIG. 2. Nonpolarized Raman spectra of FePSe_3 (top) and FePS_3 (bottom) recorded at 5 K in quasibackscattering geometry on the x - y plane. The 514.5- and 488.0-nm lines of an argon-ion laser were used for selenide and sulfide, respectively.

In Fig. 2 we present the nonpolarized Raman spectrum of FePSe_3 and FePS_3 recorded at 5 K with $\lambda = 514.5$ and 488 nm, respectively. The low-frequency spectrum (from 0 to ≈ 500 and 580 cm^{-1} for FePSe_3 and FePS_3 , respectively) has been satisfactorily interpreted in terms of vibrational modes.⁷⁻⁹ The high-frequency part of the spectra at liquid-helium temperature is shown in Fig. 3 in polarized conditions.

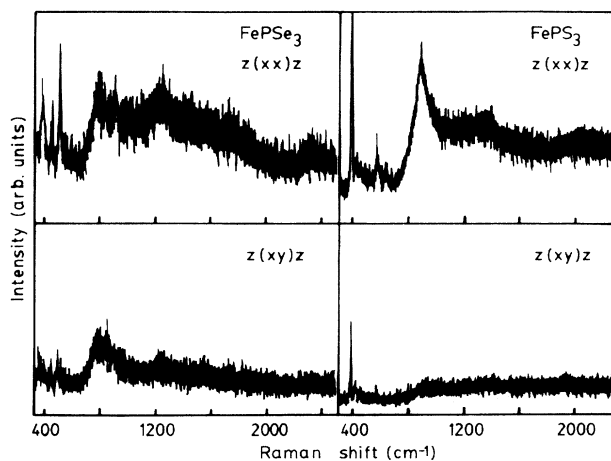


FIG. 3. Polarized Raman spectra of FePSe_3 (left) and FePS_3 (right) recorded at 5 K with the 476.5- and 488.0-nm lines of an argon-ion laser, respectively.

TABLE I. Position of the bands at frequencies above 600 cm^{-1} at 5 K (in cm^{-1}) observed by Raman scattering.

	Observed frequencies			
FePS_3	885		1400	1900
FePSe_3	800	900	1230	1710

Because of the high refractive index of these materials, the experimental arrangement corresponds to a quasi-backscattering geometry, in which only polarization perpendicular to the c axis can be achieved. The scattered light is analyzed by selecting the component whose polarization is either parallel to perpendicular to that of the incident laser beam.

The high-frequency spectra show some distinctive features: a weak, broadband extending from ≈ 600 to 2000 cm^{-1} , over which some structure of narrower bands (though still broader than the phonon peaks) is resolved. The frequencies of all the features appearing in this region of the spectrum are listed in Table I.

Several facts permit us to exclude phonons as the origin of these bands and assign them to electronic Raman transitions: First, their frequency is much higher than typical phonon frequencies.⁸ Second, the line shapes, unlike phonon peaks, are broad and have very low peak intensity, as seen in Fig. 2. Third, their temperature evolution is atypical: As the temperature is raised, they decrease slowly and above 100 K disappear completely, both in FePS_3 and FePSe_3 . Finally, comparison of results from different MPX_3 compounds shows that, except for some low-frequency peaks involving metal vibrations, all the other phonon peaks appear approximately at the same frequencies upon changing the transition metal.⁷ On the contrary, the high-frequency spectrum that we are considering depends drastically on M , being quite similar, for instance, in FePS_3 and FePSe_3 , but completely different in Ni, Mn, or Zn compounds. Spectra resembling ours, though at lower frequency ($500\text{--}600 \text{ cm}^{-1}$), have been observed in iron dichloride and dibromide and assigned to Fe^{2+} electronic Raman transitions.¹⁰ In FeF_2 , the Fe^{2+} spectrum has been identified at 1082 cm^{-1} .^{11,12} This allows us to identify the Fe^{2+} electronic structure as the origin of our bands.

There is another possibility which may relate the spectrum to the magnetic ordering at low temperatures. Both compounds undergo a phase transition from paramagnetic to antiferromagnetic order, with $T_N=112$ and 116 K for FePSe_3 and FePS_3 , respectively. In the antiferromagnetic phase, ferromagnetic chains are coupled antiferromagnetically in each layer and also with neighboring chains in adjacent layers¹³ (see Fig. 1). The one-magnon Raman peak has been found at low temperature at 114 cm^{-1} in FePSe_3 (Ref. 14) and 121 cm^{-1} in FePS_3 .¹⁵ It may be suggested that the spectrum under consideration could be the two-magnon spectrum, which in antiferromagnetic compounds can be much stronger than the one-magnon peak.¹⁶ The large difference between the position of the band (about 800 cm^{-1}) and twice the one-magnon frequency would be due to the dispersion in the magnon branch and the fact that the double-magnon

spectrum peaks near zone boundaries. This model would explain the disappearance of the spectrum at high temperature, but presents, however, several problems: First, in compounds with quasi-two-dimensional magnetic character, the double-magnon spectrum is usually seen quite above T_N .¹⁷ This is not the case in our samples. Second, the frequency shift toward lower values as T is increased, typical of peaks of magnetic origin, is not observed. Finally, even considering the dispersion of the magnon branch, the frequency is too high, compared with typical values of other transition-metal layered compounds.¹⁸

The polarization behavior of FePSe_3 and FePS_3 is different, as can be seen in Fig. 3: The broadband appearing between 600 and 2000 cm^{-1} , as well as the remaining background, is mainly polarized in parallel configuration in both compounds. The behavior of the other bands superposed to the large one, on the contrary, differs. In selenide the first band (800 cm^{-1}), when measured with respect to the background, is depolarized, while the other two (1230 and 1710 cm^{-1}) are only partially polarized in parallel. The band at 900 cm^{-1} in FePSe_3 , well above the range of phonon modes, is due to a double phonon.¹⁹ In sulfide all the features seem to be polarized in parallel, though a weak background is still seen in perpendicular polarization.

III. CRYSTAL-FIELD THEORY

In this section we summarize the model based on crystal-field potentials adapted to the site symmetry of Fe^{2+} and present the calculation of the probability of electronic Raman transitions within the low-lying iron states.

A. Hamiltonian terms

In the quasimolecular approach, only the Fe^{2+} ion and its immediate surroundings are considered. As shown in Fig. 1, the six chalcogens around Fe form a quasioctahedral cage, with the $[111]$ axis parallel to the crystal c axis. The octahedron is trigonally elongated in both FePS_3 and FePSe_3 , resulting in a D_{3d} local symmetry for iron at room temperature. On lowering the temperature, the phase transition is accompanied in FePS_3 by a magnetostriction effect which lowers the site symmetry of iron from trigonal to monoclinic (C_{2h}), as shown by x-ray diffraction.²⁰ No such magnetostriction phenomenon has been found in FePSe_3 .¹³

The electronic Hamiltonian for Fe^{2+} ($3d^6$ configuration) is written as

$$H = H_{\text{FI}} + H_{\text{CF}} + H_{\text{SO}}, \quad (1)$$

where the free-ion Hamiltonian H_{FI} contains the kinetic energy of the electrons, the Coulomb interaction with the nucleus, and the interelectronic repulsion; the result of all these terms is to give a 5D term ($L=2, S=2$) as the multielectronic ground state. H_{CF} stands for the crystal-field potential, and the spin-orbit coupling term H_{SO} is given by $H_{\text{SO}} = \lambda \mathbf{L} \cdot \mathbf{S}$, λ being the spin-orbit coupling constant. H_{CF} contains, in order of importance, a cubic term (H_C),

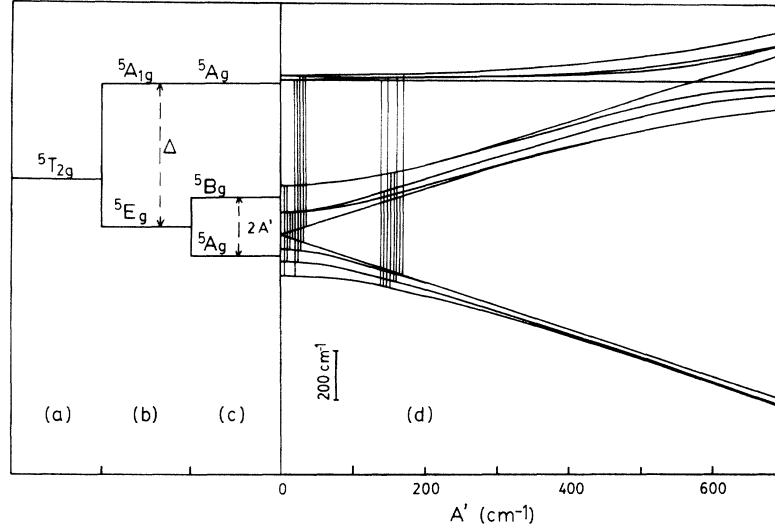


FIG. 4. Electronic-level diagram of the 5D term of Fe^{2+} split by the (a) cubic, (b) trigonal, and (c) monoclinic components of crystal field. Only the states arising from the cubic ${}^5T_{2g}$ are shown. The effect of spin-orbit coupling is shown in (d), where the allowed transitions are indicated by vertical lines for FePSe_3 (left) and FePS_3 (right).

the trigonal distortion (H_T), and, for FePS_3 , the monoclinic term (H_{MC}) arising from the magnetostriction effect.

Because of the predominantly trigonal symmetry, we have chosen a reference system with $z \parallel [111]$ and x, y in the layer plane. H_C splits the 5D term into ${}^5T_{2g}$ and 5E_g states, the triplet being lower for the d^6 configuration. As the energy separation between these levels, $10Dq$, is very large ($\approx 9000 \text{ cm}^{-1}$) compared with the magnitude of H_T , H_{SO} , and H_{MC} , the mixing of E_g states with T_{2g} states through these perturbations will be negligible and an effective angular momentum approach for T_{2g} is justified. In this case we define L' with $L'=1$ such that, within triplet states, $\langle L' \rangle = -\langle L \rangle$. Then we write the spin-orbit coupling as $H_{SO} = -\lambda L'S$ and the trigonal term as

$$H_T' = \Delta[(L_z')^2 - L'(L'+1)/3], \quad (2)$$

with an effective trigonal parameter Δ . H_T' splits the ground T_{2g} into a doublet E_g and a singlet A_{1g} , with energies $\Delta/3$ and $-2\Delta/3$, respectively.

The monoclinic term H_{MC} accounts for the deformation of the sulfur cage in FePS_3 at $T < T_N$, which leaves the crystallographic b direction as monoclinic axis ($C_2 \parallel b$). We choose our reference system in the layer such that $x \parallel a$ and $y \parallel b$. With respect to these axes, we write the general form of a crystal-field potential compatible with C_{2h} symmetry in T_{2g} subspace as

$$H_{MC}' = A'(L_2'^2 + L_{-2}'^2) + B'(L_1'^2 - L_{-1}'^2), \quad (3)$$

where $L_q'^2$ are irreducible tensor operators constructed out of L_x', L_y', L_z' . A monoclinic term of form (3) splits the lower trigonal doublet into two singlets A_g and B_g , the splitting being $2A'$; the effect of B' is to mix the lower and upper A_g states. For small distortion this effect will be small, and this term will be neglected in the subsequent treatment. In Fig. 4 we show the energy-level

scheme that derives from a Hamiltonian including H_C , H_T' , H_{MC}' , and H_{SO} .

B. Intensity calculations

The electronic Raman transition probability between two states $|i\rangle, |f\rangle$ is proportional to the square of

$$\frac{\langle f | (\mathbf{e}_s \cdot \mathbf{P})(\mathbf{e}_0 \cdot \mathbf{P}) | i \rangle}{\Delta E},$$

where \mathbf{e}_0 and \mathbf{e}_s stand for the incident- and scattered-light polarizations, respectively, \mathbf{P} is the total electronic momentum, and ΔE is a typical energy difference between the initial and intermediate states.²¹ Because of the experimental conditions, $\mathbf{e}_0, \mathbf{e}_s$ lie in the x, y plane. Then we only need the quantities $\langle f | P_\alpha P_\beta | i \rangle$ with $\alpha, \beta = x$ or y . These matrix elements can be worked out with the aid of Wigner-Eckart theorem. We have calculated the Raman spectrum with these expressions, as a function of crystal-field and spin-orbit parameters.

IV. RESULTS AND DISCUSSION

In the right-hand part of Fig. 4 we indicate with solid lines the Raman transitions expected for FePSe_3 ($A'=0$) and FePS_3 ($A' \neq 0$). Without the monoclinic distortion, the polarization of the main band at 885 cm^{-1} in FePS_3 cannot be explained (the transition from E_g to A_{1g} is nonpolarized in the xy plane). Trigonal distortion and spin-orbit coupling are enough to explain the presence of the nonpolarized band at $\approx 800 \text{ cm}^{-1}$ in FePSe_3 . The crystal-field parameters can be determined from the experimental position and the I_{xy}/I_{xx} ratio. In FePSe_3 , the main band is not polarized (thus $A'=0$) and its position is given by $|\Delta| + 2|\lambda|$ in first order. In FePS_3 , the position depends also on A' . Further, the polarization ratio I_{xy}/I_{xx} is a function of λ/A' only. From the experimental result in FePS_3 , $I_{xy}/I_{xx} \approx 20\%$, we determine

TABLE II. Crystal-field parameters resulting from the fitting of the electronic Raman spectrum (in cm^{-1}). Δ stands for the trigonal parameter, A' is the monoclinic parameter, and λ is the spin-orbit coupling constant. The values for Δ correspond to the choice $\lambda = -85 \text{ cm}^{-1}$ and $A' = 190 \text{ cm}^{-1}$.

	Δ	A'	$ \lambda , \lambda < 0$
FePS_3	-580	≤ 190	≤ 85
FePSe_3	-550	0	≤ 85

$\lambda/A' = -0.45$. The $A_g \rightarrow B_g$ transition, of energy $2A'$ in first order, is not observed, most probably because it falls within the range of phonon energies, and so we must have $2A' \leq 380 \text{ cm}^{-1}$ or $A' \leq 190 \text{ cm}^{-1}$. Thus we obtain $|\lambda| \leq 85 \text{ cm}^{-1}$. For free Fe^{2+} , $|\lambda|$ is 103 cm^{-1} .²² The decrease of $|\lambda|$ from this value is considered to be due to covalency effects. With the choice of $\lambda = -85 \text{ cm}^{-1}$, we obtain $A' = 190 \text{ cm}^{-1}$ and $\Delta = -580 \text{ cm}^{-1}$ for FePS_3 . For FePSe_3 , we obtain $\Delta = -550 \text{ cm}^{-1}$, assuming the same λ . It is to be noted that $\lambda = -85 \text{ cm}^{-1}$ has also been obtained in $\text{Fe}_{1-x}\text{Zn}_x\text{F}_2$.²³ The crystal-field parameters resulting from the fitting are given in Table II.

The possibility of a thermal population of low-lying states close to the ground state has been taken into account by superposing the spectra arising from the first five levels, weighted by the Boltzmann factor, and normalizing with the temperature-dependent partition function. A linewidth has been added in order to reproduce the experimental spectra. The result for $T = 10 \text{ K}$ is shown in Fig. 5. We now discuss the main aspects of our results.

(i) Number of bands: Only one intense band appears in the calculation with no bands at frequencies higher than 1000 cm^{-1} . There are, however, bands observed experimentally at 1230 and 1710 cm^{-1} in FePSe_3 and at 1400 and 1900 cm^{-1} in FePS_3 . We have interpreted these bands as the first and second phonon sidebands of the main electronic band, resulting from interaction with the E_g phonon at 450 cm^{-1} , for FePSe_3 , and with the A_{1g} phonon at 573 cm^{-1} in FePS_3 . A similar model has been proposed to explain the electronic spectrum of FeF_2 .¹²

(ii) Width of the bands and background of the spectrum: Two contributions are presumably broadening the bands: The first contribution is the coupling with the lattice. Besides the specific coupling with the modes producing the phonon sidebands, the coupling with other lattice vibrations can be strong. This is supported, for instance, by the presence of a Jahn-Teller effect in the E_g excited state²⁴ or the magnetoelastic coupling at temperatures below T_N .²⁰ Second, we are employing a quasi-molecular approach which gives rise to narrow, localized states, whereas electronic-structure calculations predict a certain width for d bands, with participation of, mainly, chalcogen states.⁴

(iii) Temperature evolution: Though the calculations predict a broadening of the band as a consequence of the excited-state population, the disappearance observed as the temperature is raised cannot be explained within our model.²⁵ We now discuss several possibilities to explain this evolution.

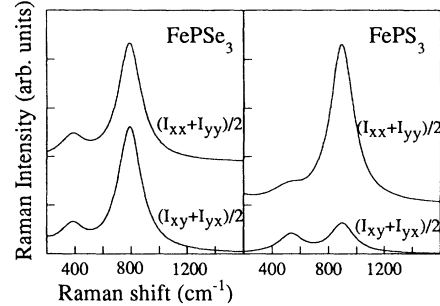


FIG. 5. Calculated electronic Raman spectrum of FePSe_3 and FePS_3 at $T = 10 \text{ K}$.

(a) Magnetic origin: The coincidence of the temperature at which the spectrum is lost with T_N suggests that magnetism may have something to do with this phenomenon. There is another case showing similar behavior: In antiferromagnetic FeF_2 ,¹¹ two models have been proposed to explain the disappearance of the electronic Raman band at 1000 cm^{-1} with increasing temperature. First, it has been suggested that the excited state participating in the Raman process could be of magnetic origin. The other mechanism proposed for FeF_2 assigns the band at 1000 cm^{-1} to a magnon-assisted electronic transition. Since t_{2g} orbitals are strongly coupled in Fe-Fe direct exchange interaction, this model seems quite plausible. We note that our model is based on a single-ion calculation, so that it cannot account for collective phenomena such as magnetism or magnetically activated features.

(b) Effect of resonance: We may also attribute the decreasing intensity to a variation in resonance conditions. In fact, the spectrum of both compounds presents some resonance enhancement toward longer wavelengths when using argon-laser lines. The region corresponds to spin-allowed intra- d -band transitions, whose oscillator strength decreases slightly from 80 K to room temperature.⁵ We think that this may partially explain the reduction but not the disappearance of the electronic Raman spectrum.

V. CONCLUSION

We have performed a study of the Fe^{2+} electronic Raman spectrum. The validity of the model based on crystal-field potential seems to be justified, though some aspects remain unexplained, mainly those concerning the temperature evolution of the spectrum and the nature of the large background. The different polarization results obtained for FePS_3 and FePSe_3 have been explained as a consequence of the lower symmetry of the iron site in the former, caused by a magnetostriction effect below T_N .

ACKNOWLEDGMENTS

We are indebted to G. Ouvrard and R. Brec from the Laboratoire de Chimie des Solides, Nantes, France, for providing us the samples.

- *Permanent address: Instituto de Ciencia de Materiales de Aragón, Universidad de Zaragoza-CSIC, Facultad de Ciencias, 50009 Zaragoza, Spain.
- ¹R. Brec, G. Ouvrard, and J. Rouxel, *Mater. Res. Bull.* **20**, 1257 (1985); G. Ouvrard, R. Brec, and J. Rouxel, *ibid.* **20**, 1181 (1985).
 - ²M. H. Whangbo, R. Brec, G. Ouvrard, and J. Rouxel, *Inorg. Chem.* **24**, 2459 (1985).
 - ³See, for a review, R. Brec, *Solid State Ion.* **22**, 3 (1986), and references cited therein.
 - ⁴H. Mercier, Ph.D. thesis, Université de Paris Sud-Orsay, 1985; H. Mercier, Y. Mathey, and E. Canadell, *Inorg. Chem.* **26**, 963 (1987).
 - ⁵M. Piacentini, F. S. Khumalo, G. Leveque, C. G. Olson, and D. W. Lynch, *Chem. Phys.* **72**, 61 (1982); M. Piacentini, F. S. Khumalo, C. G. Olson, J. W. Anderegg, and D. W. Lynch, *Chem. Phys.* **65**, 289 (1982).
 - ⁶J. Zaanen, G. Sawatzky, and J. W. Allen, *Phys. Rev. Lett.* **55**, 418 (1985).
 - ⁷C. Sourisseau, J. P. Forgerit, and Y. Mathey, *J. Solid State Chem.* **49**, 134 (1983).
 - ⁸M. Bernasconi, G. L. Marra, G. Benedek, L. Miglio, M. Jouanne, C. Julien, M. Scagliotti, and M. Balkanski, *Phys. Rev. B* **38**, 12089 (1988).
 - ⁹M. Scagliotti, M. Jouanne, M. Balkanski, G. Ouvrard, and G. Benedek, *Phys. Rev. B* **35**, 7097 (1987).
 - ¹⁰I. W. Johnstone, D. J. Lockwood, and G. Mischler, *J. Phys. C* **11**, 2147 (1978).
 - ¹¹S. R. Chinn and H. J. Zeiger, in *Magnetism and Magnetic Materials 1971 (Chicago)*, Proceedings of the 17th Annual Conference on Magnetism and Magnetic Materials, edited by D. C. Graham and J. J. Rhyne, AIP Conf. Proc. No. 5 (AIP, New York, 1972).
 - ¹²D. H. Boal, J. T. Hoff, P. Grunberg, J. Preudhomme, and J. A. Koningstein, *Raman Spectrosc.* **1**, 489 (1973).
 - ¹³G. Le Flem, R. Brec, G. Ouvrard, A. Louisy, and P. Segransan, *J. Phys. Chem. Solids* **43**, 455 (1982).
 - ¹⁴M. Jouanne, M. A. Kanehisa, C. Julien, and T. Sekine (unpublished).
 - ¹⁵T. Sekine, M. Jouanne, C. Julien, and M. Balkanski, *Phys. Rev. B* **42**, 8382 (1990).
 - ¹⁶P. A. Fleury and R. Loudon, *Phys. Rev.* **166**, 514 (1968).
 - ¹⁷P. A. Fleury and H. J. Guggenheim, *Phys. Rev. Lett.* **24**, 1346 (1970).
 - ¹⁸D. J. Lockwood, in *Light Scattering in Solids III*, edited by M. Cardona and G. Güntherodt, Vol. 51 of Springer Topics in Applied Physics (Springer-Verlag, Berlin, 1982).
 - ¹⁹M. Jouanne and C. Julien, *J. Appl. Phys.* **64**, 3637 (1988).
 - ²⁰P. Jernberg, S. Bjarmans, and R. Wäppling, *J. Magn. Magn. Mater.* **46**, 178 (1984).
 - ²¹Very near the resonance, the symmetry of the intermediate state must be taken into account. As different intermediate states may be involved, a different factor may affect the transition probability, depending on polarization conditions.
 - ²²S. Sugano, Y. Tanabe, and H. Kamimura, *Multiplets of Transition Metal Ions in Crystals* (Academic, New York, 1970).
 - ²³C. B. de Araujo, *Phys. Rev. B* **22**, 266 (1980).
 - ²⁴M. Jouanne, M. L. Sanjuán, M. A. Kanehisa, M. Balkanski, and M. Scagliotti, *Mater. Sci. Eng. B* **3**, 85 (1989).
 - ²⁵It is noteworthy that a similar evolution is observed below T_N for some phonon peaks, which has been attributed to spin-dependent activations. See, for instance, Ref. 9.